

# HyFusion: Enhanced Reception Field Transformer for Hyperspectral Image Fusion

Chia-Ming Lee<sup>✉\*</sup>, Yu-Fan Lin<sup>✉\*</sup>, Yu-Hao Ho<sup>✉†</sup>, Li-Wei Kang<sup>✉†</sup>, Chih-Chung Hsu<sup>✉\*</sup>,

<sup>\*</sup>National Cheng Kung University, Tainan, Taiwan (R.O.C.)

{zuw408421476@gmail.com, aas12as12as12tw@gmail.com, cchsu@gs.ncku.edu.tw}

<sup>†</sup>National Taiwan Normal University, Tainan, Taiwan (R.O.C.)

{i0981526423@gmail.com, lwkang@ntnu.edu.tw}

**Abstract**—Hyperspectral image (HSI) fusion addresses the challenge of reconstructing High-Resolution HSIs (HR-HSIs) from High-Resolution Multispectral images (HR-MSIs) and Low-Resolution HSIs (LR-HSIs), a critical task given the high costs and hardware limitations associated with acquiring high-quality HSIs. While existing methods leverage spatial and spectral relationships, they often suffer from limited receptive fields and insufficient feature utilization, leading to suboptimal performance. Furthermore, the scarcity of high-quality HSI data highlights the importance of efficient data utilization to maximize reconstruction quality. To address these issues, we propose HyFusion, a novel framework designed to enhance the receptive field and enable effective feature map reusing, thereby maximizing data utilization. First, HR-MSI and LR-HSI inputs are concatenated to form a quasi-fused draft, preserving complementary spatial and spectral details. Next, the Enhanced Reception Field Block (ERFB) is introduced, combining shifting-window attention and dense connections to expand the receptive field, effectively capturing long-range dependencies and reusing features to reduce information loss, thereby boosting data efficiency. Finally, the Dual-Coupled Network (DCN) dynamically extracts high-frequency spectral and spatial features from LR-HSI and HR-MSI, ensuring efficient cross-domain fusion. Extensive experiments demonstrate that HyFusion achieves state-of-the-art performance in HR-MSI/LR-HSI fusion, significantly improving reconstruction quality while maintaining a compact model size and computational efficiency. By integrating enhanced receptive fields and feature map reusing, HyFusion provides a practical and effective solution for HSI fusion in resource-constrained scenarios, setting a new benchmark in hyperspectral imaging. Our code will be publicly available.

**Index Terms**—Hyperspectral Image Fusion, Hyperspectral Image Pansharping, Transformer, Reception Field, Data Efficiency

## I. INTRODUCTION

Hyperspectral imaging (HSI) captures detailed spectral information for every pixel in an image, providing a significantly broader spectral range compared to conventional imaging techniques, with channels ranging from tens to hundreds. This unique capability has enabled diverse applications across fields such as science, military, agriculture, and medicine [1]. However, HSI sensing systems face notable hardware constraints, particularly in miniaturized satellites and resource-limited platforms. These constraints limit the achievable spectral and spatial resolutions. As a result, capturing high-quality, high-resolution hyperspectral images (HR-HSI) is both technically

challenging and financially costly, particularly for resource-constrained platforms such as small satellites. Consequently, data scarcity poses a significant hurdle for the practical deployment of many HSI applications.

One widely adopted solution to address these limitations is to capture high-resolution multispectral images (HR-MSIs) alongside low-resolution hyperspectral images (LR-HSIs). Fusion-based super-resolution (SR) techniques [2–4] combine HR-MSIs and LR-HSIs to reconstruct high-resolution hyperspectral images (HR-HSIs). These techniques have proven effective in overcoming resolution limitations and maximizing the utility of limited HSI data [5–9].

Despite their effectiveness, HSI fusion tasks remain inherently challenging, as they require the seamless integration of spatial and spectral information while preserving fine spectral details and enhancing spatial resolution. Existing methods often face two major challenges. First, the loss of critical spatial and spectral information as network depth increases. Second, the underutilization of rich spatial-spectral relationships in the input data. This information loss is particularly problematic in HSI applications, where making the most of the limited available data is crucial due to the scarcity of high-quality HSI datasets. While deep learning (DL)-based HSI fusion methods [10–13] have advanced the field, many state-of-the-art techniques fail to fully address key challenges such as receptive field expansion and feature map reuse. Consequently, these methods often fall short in maximizing data utilization, which compromises their overall fusion performance. Furthermore, the computational and hardware limitations inherent to HSI applications demand solutions that are not only highly effective but also efficient and easy to implement.

To overcome these challenges, we propose HyFusion, a novel framework designed to enhance the receptive field and reuse feature maps, enabling more efficient data utilization and improved HR-HSI reconstruction. The receptive field plays a crucial role by capturing long-range dependencies and spatial-spectral correlations, as illustrated in Figure 1. While feature map reuse, facilitated by dense connections, retains and amplifies extracted information throughout the network. At the core of HyFusion is the Enhanced Reception Field Block (ERFB), which integrates Improved Swin Transformer Layers (ISTL) with dense connections to expand the receptive field and preserve critical spatial-spectral features, addressing

(Corresponding author: Chih-Chung Hsu; Email: cchsu@gs.ncku.edu.tw)

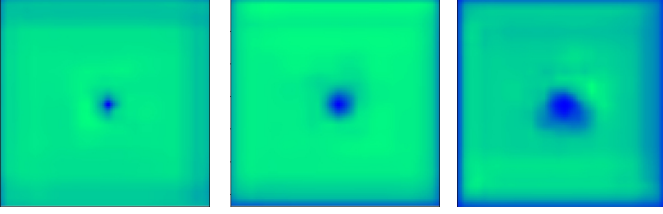


Fig. 1. Visualization of Effective Reception Field. (a) naive Swin Transformer Layer (STL), (RSTB in deep feature extraction [14]); (b) with dense connection (using RDG [15]); (c) with dense connection and improved STL (Ours).

the limitations of existing methods by mitigating information loss and enhancing feature retention. Additionally, HyFusion introduces a Dual-Coupled Network (DCN) comprising two specialized networks: SpeNet, for extracting spectral features, and SpaNet, for extracting spatial features. To guide network convergence, we employ task-specific spectral-aware and frequency-aware loss functions, which align reconstructed HR-HSIs with ground-truth in both frequency and spatial-spectral domains, ensuring enhanced fidelity and minimizing artifacts in the final reconstructions.

In summary, our key contributions are as follows:

- We propose the HyFusion framework, which emphasizes Enhanced Reception Field and Feature Map Reusing through the proposed ERFB, enabling the network to maximize data utilization by capturing long-range dependencies and reusing extracted features across layers.
- The proposed DCN dynamically integrates spectral and spatial features from HR-MSI and LR-HSI, leveraging dense connections to fully exploit limited data while maintaining a simple and efficient network architecture.
- We design task-specific loss functions to ensure alignment between reconstructed HR-HSIs and ground truth in both frequency and spatial-spectral domains, improving fidelity and eliminating artifacts.

By integrating enhanced receptive fields and feature map reusing into the fusion process, HyFusion effectively addresses the challenges of data scarcity and information loss, establishing a new benchmark for efficient and high-quality HSI fusion in resource-constrained environments.

## II. PROPOSED METHOD

### A. Architecture of Proposed HyFusion

To design an efficient LR-HSI/HR-MSI fusion model, we aim to use dense-connections [16] to minimize the loss of valuable spectral and spatial information during fusion and enhance the receptive field, thereby ensuring effective information complementarity and high-quality HR-HSI reconstruction. However, cross-domain information fusion requires effective interaction while considering the high computational and hardware resource consumption due to the large size of HSI. Thus, the network architecture must be simple, efficient, and effective for practical applications.

Inspired by ensemble learning in traditional machine learning, which enhances classification performance by using two simple independent classifiers for different modalities and combining their results through voting or weighted averaging,

our DCN leverages these advantages. Specifically, we fully exploit the input’s spectral and spatial information by designing two distinct subnetworks to aggregate the information, thereby improving fusion performance with lower computational and spatial complexity.

This section illustrates the architectural design of our DCN, as shown in Figure 2, including the spatial and spectral perception networks (SpaNet and SpeNet) for LR-HSI and HR-MSI. To effectively combine the features of LR-HSI and HR-MSI, the proposed SpaNet and SpeNet not only extract their corresponding feature representations but also utilize early image fusion to allow the corresponding counterparts to provide guidance simultaneously. This approach allows us to seamlessly integrate spatial and spectral feature representations without increasing model complexity.

### B. Proposed Dual-Coupled Network

Let the LR-HSI and HR-MSI be  $\mathbf{X}_h \in \mathbb{R}^{h_h \times w_h \times b}$  and  $\mathbf{X}_m \in \mathbb{R}^{h_m \times w_m \times b_m}$ . The observable LR-HSI can be modeled as  $\mathbf{X}_h = \mathbf{Y}\mathbf{B}$ , where  $\mathbf{B}$  is a blurring matrix that reduces the pixel count. Similarly, the observable HR-MSI is given by  $\mathbf{X}_m = \mathbf{D}\mathbf{Y}$ , where  $\mathbf{D}$  is a downsampling matrix that decreases the number of spectral bands.

The reconstructed HR-HSI denotes  $\mathbf{Y}^* \in \mathbb{R}^{w \times h \times b}$  by:

$$\mathbf{Z}_{hm} = f_{\text{DCN}}(\mathbf{X}_h, \mathbf{X}_m) = \text{Concat.}(\mathbf{Z}_h, \mathbf{Z}_m), \quad (1)$$

where the high-spectral-resolution and high-spatial-resolution features are obtained as:

$$\mathbf{Z}_h = f_{\text{SpeNet}}(\mathbf{X}_h, \mathbf{X}_m); \mathbf{Z}_m = f_{\text{SpaNet}}(\mathbf{X}_m, \mathbf{X}_h) \quad (2)$$

For SpeNet, we up-sample the LR-HSI to obtain  $\mathbf{X}_h^u = f_{\text{up}}(\mathbf{X}_h)$ , where  $f_{\text{up}}$  denotes the bilinear interpolation function. Then, the quasi-spectral draft is obtained by:

$$\mathbf{Z}_h' = \text{Concat.}(\mathbf{X}_h^u, \mathbf{X}_m) \quad (3)$$

Similarly for SpaNet, we down-sample the HR-MSI to obtain  $\mathbf{X}_m^d = f_{\text{down}}(\mathbf{X}_m)$ , where  $f_{\text{down}}$  denotes the bicubic interpolation function, creating a quasi-spatial draft:

$$\mathbf{Z}_m' = \text{Concat.}(\mathbf{X}_h, \mathbf{X}_m^d) \quad (4)$$

After obtaining these preliminary drafts, shallow feature extraction is performed using  $3 \times 3$  convolution with LeakyReLU activation (negative slope 0.2). The ERFB is then used for deep feature extraction, with skip-connections enhancing feature quality and stabilizing training. The reconstructed HR-HSI is:

$$\mathbf{Y}^* = f_{\text{Rec}}(\mathbf{Z}_{hm}) \quad (5)$$

### C. Enhanced Reception Field Block

Given the inherent data scarcity in hyperspectral imaging due to hardware limitations and acquisition costs, maximizing the utility of limited available data becomes crucial. The proposed ERFB is specifically designed to address this challenge along with two fundamental issues in hyperspectral image fusion: capturing comprehensive spatial-spectral relationships through long-range dependencies and maximizing feature utilization efficiency. By effectively reusing features

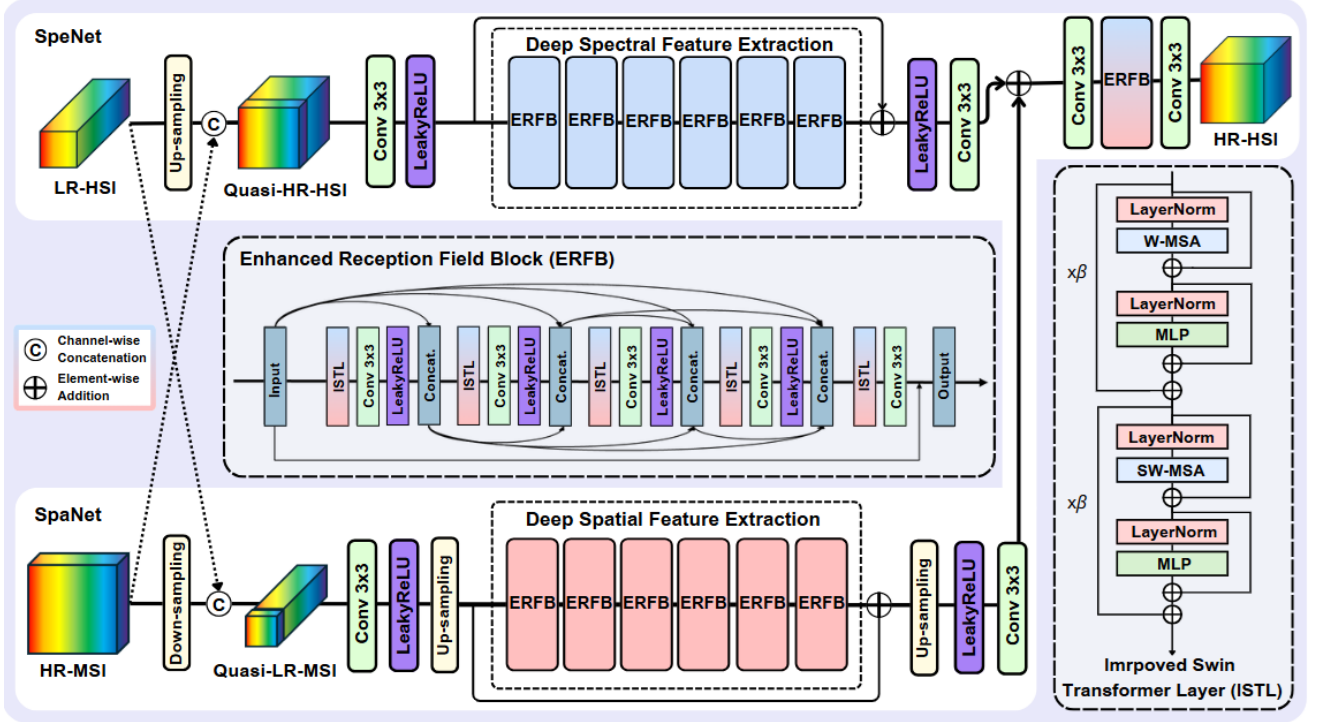


Fig. 2. The proposed HyFusion network architecture integrates an Enhanced Reception Field Block (ERFB) with an Improved Swin Transformer Layer (ISTL) for HSI/MSI fusion. Through our Dual-Coupled Network (DCN), the architecture learns spatial-spectral representations across two specialized branches. The combination of ERFB, ISTL and DCN enables effective capture of long-range dependencies while maintaining streamlined design, leading to superior fusion results through efficient information exchange between spatial and spectral domains, thereby improving data efficiency for HSI real-world applications.

TABLE I

PERFORMANCE EVALUATION AND COMPLEXITY COMPARISON OF THE PROPOSED METHOD AND OTHER FUSION MODELS. THE BEST RESULTS ARE HIGHLIGHTED IN **BOLD-RED**, WHILE THE SECOND-BEST RESULTS ARE HIGHLIGHTED IN **BOLD-BLUE**. ROWS ARE COLORED TO DISTINGUISH DIFFERENT APPROACHES: CNN-BASED , TRANSFORMER-BASED , AND THE PROPOSED METHODS.

Method	#Params $\downarrow$	Complexity			4 Bands LR-HSI				6 Bands LR-HSI			
		FLOPs $\downarrow$	Run-time $\downarrow$	Memory $\downarrow$	PSNR $\uparrow$	SAM $\downarrow$	RMSE $\downarrow$	ERGAS $\downarrow$	PSNR $\uparrow$	SAM $\downarrow$	RMSE $\downarrow$	ERGAS $\downarrow$
<b>PZRes-Net</b> [17] TIP' 21	40.15M	5262G	0.0141s	11059MB	34.963	1.934	35.498	1.935	37.427	1.478	28.234	1.538
<b>MSSJFL</b> [18] HPCC' 21	16.33M	175.56G	<b>0.0128s</b>	<b>1349MB</b>	34.966	1.792	33.636	2.245	38.006	1.390	26.893	1.535
<b>Dual-UNet</b> [19] TGRS' 21	<b>2.97M</b>	<b>88.65G</b>	<b>0.0127s</b>	<b>2152MB</b>	<b>35.423</b>	1.892	33.183	<b>1.796</b>	38.453	1.548	26.148	1.205
<b>DHIF-Net</b> [20] TCI' 22	57.04M	13795.11G	6.005s	29381MB	34.458	1.829	34.769	2.613	<b>39.146</b>	1.239	25.309	<b>1.113</b>
<b>FusFormer</b> [21] TGRS' 22	<b>0.18M</b>	<b>11.74G</b>	0.0158s	5964MB	34.217	2.012	35.687	1.996	38.637	1.678	28.674	1.204
<b>HyperTransformer</b> [22] CVPR' 22	142.83M	343.96G	0.0252s	8104MB	28.692	3.664	62.231	4.774	32.954	2.568	41.256	3.834
<b>HyperRefiner</b> [23] TJDE' 23	19.32M	94.37G	0.0237s	7542MB	33.298	2.129	38.769	2.086	37.654	1.590	29.629	1.403
<b>QRCODE</b> [24] TGRS' 24	41.88M	2231.19G	0.2452s	15028MB	35.361	<b>1.623</b>	<b>32.711</b>	2.027	38.948	<b>1.148</b>	<b>24.617</b>	1.429
<b>HyFusion (Ours)</b>	25.53M	641.49G	0.0294s	2572MB	<b>37.421</b>	<b>1.256</b>	<b>27.425</b>	<b>1.172</b>	<b>40.197</b>	<b>1.017</b>	<b>21.455</b>	<b>1.076</b>

and enhancing the receptive field, ERFB enables the network to learn robust representations even with limited training data.

Our design philosophy centers on a dual-enhancement strategy that synergistically combines dense connections for thorough feature reuse with an ISTL for enhanced receptive field and long-range dependency modeling. The dense connection structure ensures that each layer can access and build upon all previous feature representations, effectively preventing information loss and vanishing gradients that commonly occur in deep networks. This is particularly crucial for hyperspectral image fusion, where preserving fine spectral details while maximizing the utility of limited data is essential.

At the core of our ERFB is the ISTL, which consists of two sequential processing paths: W-MSA and SW-MSA. Each path contains LayerNorm, attention (W-MSA or SW-MSA), LayerNorm, and MLP blocks with learnable parameters  $\beta_1$  and  $\beta_2$  respectively to adaptively control feature contributions:

$$\text{ISTL}(\mathbf{X}) = \beta_1 \cdot \text{Path}_{\text{W-MSA}}(\mathbf{X}) + \beta_2 \cdot \text{Path}_{\text{SW-MSA}}(\mathbf{X}) \quad (6)$$

The dense connection pattern in ERFB progressively accumulates and reuses features for reception field enhancement:

$$\mathbf{Z}_j = \text{ISTL}(\text{Conv}_{3 \times 3}(\text{Cat}(\mathbf{Z}_0, \dots, \mathbf{Z}_{j-1}))), j = 1, 2, 3, 4 \quad (7)$$

where  $\text{Cat}(\cdot)$  represents the channel-wise concatenation, and  $\text{Conv}_{3 \times 3}$  fuses the concatenated features with LeakyReLU activation with 0.2 negative slope. The final stage processes the accumulated features:

$$\mathbf{Z}_5 = \text{Conv}_{3 \times 3}(\text{ISTL}(\mathbf{Z}_4)) \quad (8)$$

With the efficient information flow via dense connectivity within ERFB, and adaptive feature weighting through ISTL, the long-range dependency modeling capability of the proposed HyFusion can be improved, as shown in Figure 1. In the context of limited hyperspectral training data, this architecture

proves particularly valuable as it maximizes the utility of available information through feature reuse while maintaining the ability to capture complex spatial-spectral relationships. When incorporated into both SpeNet and SpaNet branches of the DCN architecture, this approach provides a informative representations for high-quality hyperspectral image fusion while maintaining computational and data efficiency.

#### D. Task-Specific Optimization

Recognizing the paramount importance of spectral index in HSI, we introduce a Spectral Angle Mapper (SAM) loss function and Stationary Wavelet Transform (SWT) loss to guide the network:

$$\ell_{\text{SAM}} = \frac{1}{N} \sum_{n=1}^N \cos^{-1} \left( \frac{\mathbf{Y}_n^T \mathbf{Y}_n^*}{\|\mathbf{Y}_n\|_2 \cdot \|\mathbf{Y}_n^*\|_2} \right) \quad (9)$$

$$\ell_{\text{SWT}}(\mathbf{Y}, \mathbf{Y}^*) = \mathbb{E} \left[ \sum_j \lambda_j \|\text{SWT}(\mathbf{Y})_j - \text{SWT}(\mathbf{Y}^*)_j\|_1 \right] \quad (10)$$

Finally, the total loss with L1 loss can be written as:

$$\ell_{\text{Total}}(\mathbf{Y}, \mathbf{Y}^*) = \ell_1(\mathbf{Y}, \mathbf{Y}^*) + \lambda_1 \ell_{\text{SAM}}(\mathbf{Y}, \mathbf{Y}^*) + \lambda_2 \ell_{\text{SWT}}(\mathbf{Y}, \mathbf{Y}^*) \quad (11)$$

### III. EXPERIMENTAL RESULTS

#### A. Experiment Settings

1) *Dataset Illustration*: The dataset used for performance evaluation in this study was acquired by the Airborne Visible/Infrared Imaging Spectrometer (AVIRIS) sensor [25]. It consisted of 2,078 HR-HSI images, which were randomly partitioned into training, validation, and testing sets for performance evaluation. The training set contained 1,678 images, while the validation and testing sets contained 200 images for each. The spatial and spectral resolutions of the HR-MSI and LR-HSI were  $256 \times 256 \times M_m$  and  $64 \times 64 \times 172$ , respectively, where  $M_m$  is either 4 or 6 in our experiments.

2) *Implementation Details*: The proposed method was implemented using the PyTorch deep learning framework. The batch size was set to 4, and the number of training epochs was fixed to 600 for all experiments involving the proposed method. For the peer methods, the number of training epochs was set according to their default values as specified in their respectively original publications. The ADAM [26] optimizer was used for training, with an initial learning rate of 0.0001. The learning rate was adjusted during the training process using the Cosine Annealing learning decay scheduler. The weights of the penalty terms in the loss function, denoted as  $\lambda_1$  and  $\lambda_2$ , were both set to 0.01. Standard data augmentation, including random cropping and rotation, is adopted in this paper for all of the evaluated methods.

#### B. Quantitative Results

To evaluate the performance of our hyperspectral image fusion method, we compared it with five other supervised hyperspectral image fusion methods: PZRes-Net [17], MSSJFL [18], Dual-UNet [19] and DHIF-Net [20], FusFormer [21], HyperTransformer [22], HyperRefiner [23], QRCODE [24]. The

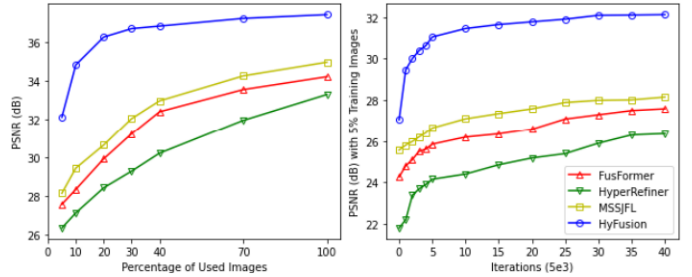


Fig. 3. Performance comparison between several HSI fusion models. (a) Evaluation of model performance with varying training data sizes. (b) Validation performance curves during training with 5% training samples.

performance was objectively measured using PSNR, SAM, and RMSE, ERGAS. Experiments were conducted with both 4 and 6 MSI bands. Table I present the results of comparing our proposed method with the state-of-the-art methods.

The experimental results demonstrate that the proposed framework outperforms the compared state-of-the-art methods in terms of spectral reconstruction performance.

#### C. Data Efficiency Analysis

To evaluate HyFusion’s ability to learn from limited training data, we conducted experiments comparing our approach with state-of-the-art methods FusFormer [21], HyperRefiner [23] and MSSJFL [18] using 4 bands LR-HSI for fusion. As shown in 3(a), we gradually reduced the percentage of training samples from 100% to 5%. HyFusion outperforms other methods by a significant margin. This demonstrates our model’s strong data efficiency, enabled by the feature reuse through dense connections and enhanced learning capability from ISTL.

The convergence analysis in 3(b) further validates HyFusion’s advantages. Our model not only achieves faster convergence but also reaches higher PSNR values throughout the training process. This rapid convergence can be attributed to the effective spatial-spectral feature extraction through our dual-branch architecture and the improved gradient flow from dense connections. The results highlight that HyFusion’s architectural innovations lead to both better performance and more efficient learning from limited hyperspectral training data.

### IV. CONCLUSION

In this paper, we have proposed HyFusion, a novel framework that effectively addresses the challenges of hyperspectral image fusion through two key innovations: the Enhanced Reception Field Block (ERFB) that integrates dense connections with an Improved Swin Transformer Layer (ISTL) for comprehensive feature utilization and stable information propagation, and a Dual-Coupled Network (DCN) architecture that enables efficient cross-domain feature extraction and data utilization for boosting data-scarce hyperspectral imagery application. Our experimental results demonstrate that HyFusion achieves state-of-the-art performance in HR-MSI/LR-HSI fusion while exhibiting remarkable data efficiency with limited training samples. The framework’s success in balancing reconstruction quality with computational efficiency makes it particularly valuable for practical hyperspectral imaging applications in resource-constrained environments.

## REFERENCES

- [1] P. Ghamisi, N. Yokoya, J. Li, W. Liao, S. Liu, J. Plaza, B. Rasti, and A. Plaza, "Advances in hyperspectral image and signal processing: A comprehensive overview of the state of the art," *IEEE Geoscience and Remote Sensing Magazine*, vol. 5, no. 4, pp. 37–78, Dec. 2017.
- [2] Y. Zhang, K. Zhang, Z. Chen, Y. Li, and R. e. a. Timofte, "Ntire 2023 challenge on image super-resolution (x4): Methods and results," in *Proceedings of the IEEE/CVF Conference on Computer Vision and Pattern Recognition (CVPR) Workshops*, June 2023, pp. 1865–1884.
- [3] B. Ren, Y. Li, N. Mehta, and R. e. a. Timofte, "The ninth ntire 2024 efficient super-resolution challenge report," in *Proceedings of the IEEE/CVF Conference on Computer Vision and Pattern Recognition (CVPR) Workshops*, June 2024, pp. 6595–6631.
- [4] Z. Chen, Z. Wu, E. Zamfir, K. Zhang, Y. Zhang, R. Timofte, and X. e. a. Yang, "Ntire 2024 challenge on image super-resolution (x4): Methods and results," in *Proceedings of the IEEE/CVF Conference on Computer Vision and Pattern Recognition (CVPR) Workshops*, June 2024, pp. 6108–6132.
- [5] R. Dian, S. Li, B. Sun, and A. Guo, "Recent advances and new guidelines on hyperspectral and multispectral image fusion," *Information Fusion*, vol. 69, pp. 40–51, 2021.
- [6] G. Vivone, "Multispectral and hyperspectral image fusion in remote sensing: A survey," *Information Fusion*, vol. 89, pp. 405–417, 2023.
- [7] X. Y. Wang, Q. Hu, Y. S. Cheng, and J. Y. Ma, "Hyperspectral image super-resolution meets deep learning: A survey and perspective," *IEEE/CAA J. Autom. Sinica*, vol. 10, no. 8, pp. 1664–1687, Aug. 2023.
- [8] C.-C. Hsu, C.-Y. Jian, E.-S. Tu, C.-M. Lee, and G.-L. Chen, "Real-time compressed sensing for joint hyperspectral image transmission and restoration for cubesat," *IEEE Transactions on Geoscience and Remote Sensing*, vol. 62, pp. 1–16, 2024.
- [9] C.-M. Lee, C.-H. Cheng, Y.-F. Lin, Y.-C. Cheng, W.-T. Liao, C.-C. Hsu, F.-E. Yang, and Y.-C. F. Wang, "Prompthsi: Universal hyperspectral image restoration framework for composite degradation," 2024. [Online]. Available: <https://arxiv.org/abs/2411.15922>
- [10] F. Palsson, J. R. Sveinsson, and M. O. Ulfarsson, "Multispectral and hyperspectral image fusion using a 3-d convolutional neural network," in *IEEE Geoscience and Remote Sensing Letters*, vol. 14, no. 5, May 2017, pp. 639–643.
- [11] W. Wang, W. Zeng, Y. Huang, X. Ding, and J. Paisley, "Deep blind hyperspectral image fusion," in *Proceedings of IEEE/CVF International Conference on Computer Vision*, Seoul, Korea, 2019.
- [12] L. Wang, C. Sun, Y. Fu, M. H. Kim, and H. Huang, "Hyperspectral image reconstruction using a deep spatial-spectral prior," in *Proceedings of IEEE/CVF Conference on Computer Vision and Pattern Recognition*, Long Beach, CA, USA, 2019, pp. 8024–8033.
- [13] Z. Min, Y. Wang, and S. Jia, "Multiscale spatial-spectral joint feature learning for multispectral and hyperspectral image fusion," in *Proceedings of IEEE International Conference on High Performance Computing Communications*, Haikou, Hainan, China, 2021, pp. 1265–1270.
- [14] J. Liang, J. Cao, G. Sun, K. Zhang, L. Van Gool, and R. Timofte, "Swinir: Image restoration using swin transformer," *arXiv preprint arXiv:2108.10257*, 2021.
- [15] C.-C. Hsu, C.-M. Lee, and Y.-S. Chou, "Drct: Saving image super-resolution away from information bottleneck," in *Proceedings of the IEEE/CVF Conference on Computer Vision and Pattern Recognition (CVPR) Workshops*, June 2024, pp. 6133–6142.
- [16] G. Huang, Z. Liu, L. Van Der Maaten, and K. Q. Weinberger, "Densely connected convolutional networks," *IEEE Transactions on Pattern Analysis and Machine Intelligence*, vol. 41, no. 8, pp. 2261–2269, 2018.
- [17] Z. Zhu, J. Hou, J. Chen, H. Zeng, and J. Zhou, "Hyperspectral image super-resolution via deep progressive zero-centric residual learning," *IEEE Transactions on Image Processing*, vol. 30, pp. 1423–1438, 2021.
- [18] Z. Min, Y. Wang, and S. Jia, "Multiscale spatial-spectral joint feature learning for multispectral and hyperspectral image fusion," in *Proceedings of IEEE International Conference on High Performance Computing Communications*, Haikou, Hainan, China, 2021, pp. 1265–1270.
- [19] J. Xiao, J. Li, Q. Yuan, and L. Zhang, "A dual-unet with multistage details injection for hyperspectral image fusion," *IEEE Transactions on Geoscience and Remote Sensing*, vol. 60, pp. 1–13, 2021.
- [20] T. Huang, W. Dong, J. Wu, L. Li, X. Li, and G. Shi, "Deep hyperspectral image fusion network with iterative spatio-spectral regularization," *IEEE Transactions on Computational Imaging*, vol. 8, pp. 201–214, 2022.
- [21] J.-F. Hu, T.-Z. Huang, L.-J. Deng, H.-X. Dou, D. Hong, and G. Vivone, "Fusformer: A transformer-based fusion network for hyperspectral image super-resolution," *IEEE Geoscience and Remote Sensing Letters*, vol. 19, pp. 1–5, 2022.
- [22] W. G. C. Bandara and V. M. Patel, "Hypertransformer: A textural and spectral feature fusion transformer for pansharpening," in *Proceedings of the IEEE/CVF Conference on Computer Vision and Pattern Recognition (CVPR)*, June 2022, pp. 1767–1777.
- [23] B. Zhou, X. Zhang, X. Chen, M. Ren, and Z. Feng, "Hyperrefiner: a refined hyperspectral pansharpening network based on the autoencoder and self-attention," *International Journal of Digital Earth*, vol. 16, no. 1, pp. 3268–3294, 2023. [Online]. Available: <https://doi.org/10.1080/17538947.2023.2246944>
- [24] C.-H. Lin, C.-C. Hsu, S.-S. Young, C.-Y. Hsieh, and S.-C. Tai, "Qrcode: Quasi-residual convex deep network for fusing misaligned hyperspectral and multispectral images," *IEEE Transactions on Geoscience and Remote Sensing*, vol. 62, pp. 1–15, 2024.
- [25] G. Vane, R. O. Green, T. G. Chrien, H. T. Enmark, E. G. Hansen, and W. M. Porter, "The airborne visible/infrared imaging spectrometer (aviris)," *Remote Sensing of Environment*, vol. 44, no. 2-3, pp. 127–143, 1993.
- [26] D. P. Kingma and J. Ba, "Adam: A method for stochastic optimization," *arXiv preprint arXiv:1412.6980*, 2014.